Ocean Engineering 276 (2023) 114230

Contents lists available at ScienceDirect

Ocean Engineering

journal homepage: www.elsevier.com/locate/oceaneng

# A data driven method for multi-step prediction of ship roll motion in high sea states

Dan Zhang [a,c,1], Xi Zhou [b,d,1], Zi-Hao Wang [b,c,*], Yan Peng [b,c], Shao-Rong Xie [e]

[a] School of Mechatronic Engineering and Automation, Shanghai University, Shanghai, 200444, China
[b] Institute of Artificial Intelligence, Collaborative Innovation Center for the Marine Artificial Intelligence, Shanghai University, Shanghai, 200444, China
[c] Engineering Research Center of Unmanned Intelligent Marine Equipment, Ministry of Education, Shanghai, 200444, China
[d] Shanghai Artificial Intelligence Laboratory, Shanghai, 200032, China
[e] School of Computer Engineering and Science, Shanghai University, Shanghai, 200444, China

ARTICLE INFO

Handling Editor: Prof. A.I. Incecik

*Keywords:*
High sea state
Multi-step predictions
Ship roll motion
Data-driven method
CNN
LSTM

ABSTRACT

Ship roll motion in high sea states has large amplitudes and nonlinear dynamics, and its prediction is significant for operability, safety, and survivability. This paper presents a novel data-driven methodology to provide a multi-step prediction of ship roll motions in high sea states. A hybrid neural network is proposed that combines long short-term memory (LSTM) and convolutional neural network (CNN) in parallel. The motivation is to extract the nonlinear dynamic characteristics and the hydrodynamic memory information through the advantage of CNN and LSTM, respectively. For the feature selection, the time histories of motion states and wave heights are selected to involve sufficient information. Taken a scaled KCS as the study object, the ship motions in sea state 7 irregular long-crested waves are simulated and used for the validation. The results show that at least one period of roll motion can be accurately predicted. Compared with the single LSTM and CNN methods, the proposed method has better performance in predicting the amplitude of roll angles. Besides, the comparison results also demonstrate that selecting motion states and wave heights as feature space improves the prediction accuracy, verifying the effectiveness of the proposed method.

## 1. Introduction

When a ship encounters high sea states, severe motion can be induced by wave-dominated environmental disturbances, significantly affecting operability, safety, and survivability. The prediction of roll motions is critical to motion compensation, which may prevent cargo crashes during the transfer and improve the aircraft landing safety on carriers and the firing accuracy of shipboard weapons systems (Huang et al., 2018). This prediction information is also helpful to captains or autopilot to make proper decisions. However, due to the complex interaction of the ship hull with the incoming waves, the accurate prediction of roll motions in high sea states is still a challenge.

Prediction approaches for ship roll motion can be broadly classified into mechanism method and data-driven method. Mechanism modeling typically establishes a mathematical model consisting of the damping moment, the restoring moment, the added moment of inertia, and the wave disturbance moment. To obtain the model parameters, model test methods (Diez et al., 2018), empirical methods (Inoue et al., 1981; Newman, 2018; Yasukawa and Yoshimura, 2015), numerical methods (Gokce and Kinaci, 2018), and system identification methods (Hou and Zou, 2016; Jiang et al., 2021; Sun et al., 2021) have been investigated. Nevertheless, the ship roll motion in high sea states has large amplitudes and belongs to typical nonlinear motion. In this case, wave disturbance moments are highly coupled with other moments, making the assumption of the conventional mechanism models invalid. Moreover, the fixed hydrodynamic coefficients are difficult to adapt to the complex and changeable ocean environment. Therefore, the conventional hydrodynamic component model is unsuitable for the accurate prediction of roll motions in high sea states (Bassler, 2013).

The data-driven modeling method extracts dynamic characteristics from the historical data. The classic time series forecast methods optimize the model structure from a prior model set, such as auto regressive

* Corresponding author. Institute of Artificial Intelligence, Collaborative Innovation Center for the Marine Artificial Intelligence, Shanghai University, Shanghai, 200444, China.

*E-mail address:* zihaowang@shu.edu.cn (Z.-H. Wang).

[1] These authors contributed equally to this work and should be considered co-first authors.

https://doi.org/10.1016/j.oceaneng.2023.114230
Received 24 July 2022; Received in revised form 23 December 2022; Accepted 16 March 2023
Available online 28 March 2023
0029-8018/© 2023 Elsevier Ltd. All rights reserved.

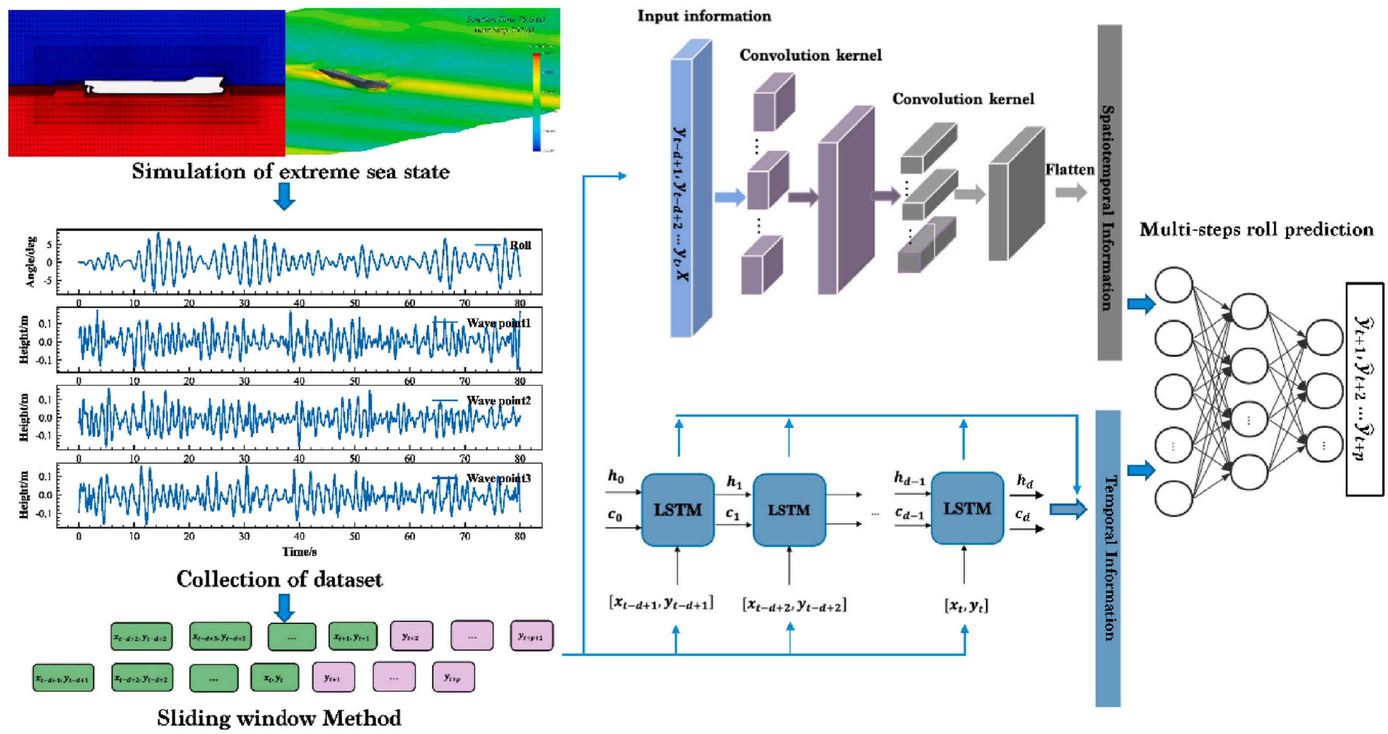


**Fig. 1.** Overview of the forecasting modeling procedure.

(AR) model and auto regressive moving average (ARMA) model (Jiang et al., 2020; Yumori, 1981). Despite high efficiency, they may not be effective for the rough sea states as the presence of stronger nonlinearity. As an alternative approach, machine learning methods have been further investigated to express the nonlinear features, which can map the input features to a high-dimensional space. Yin et al. (2013) combined radial basis function with sliding windows for ship roll motion predictions under moderate sea states. Huang et al. (2018) proposed a structural wavelet neural network for the accurate prediction of roll motion under regular waves.

It is worth noting that the ship roll motion in waves has a significant memory effect (Chung and Bernitsas, 1997; Li, 2003), that is, the hydrodynamic forces are not only related to the current states, but also to the historical states. For this issue, recurrent-type neural networks are suitable to be applied, which have good performance in time series prediction (Sutskever et al., 2014). Among them, long short-term memory (LSTM) neural networks have attracted much attention, which can overcome the gradient disappearance problem of recurrent neural networks (RNN), and improve the learning ability of long sequences by adding gating units (Hochreiter and Schmidhuber, 1997). Tang et al. (2021) adopted LSTM to predict the time series of ship motions, where the dataset under moderate sea states was simulated by wave energy spectrum and strip theory. Wei et al. (2021) employed LSTM for multi-step prediction of roll motions in moderate sea states, where the roll-motion sequence was decomposed by the adaptive empirical wavelet transform method. In general, previous studies have shown that LSTM performs well in predicting roll motions, but they mainly focus on low and moderate sea states.

For the high sea states with large amplitude of ship motions, available datasets are scarce due to the high cost and navigational safety risks. Computational fluid dynamics (CFD) based methods provide a way to get relatively realistic numerical results (Diez et al., 2018; Jiao et al., 2019; Serani et al., 2021; Wang et al., 2017). Based on the CFD data, several studies have investigated the forecast of roll motions in high sea states. Del Águila Ferrandis et al. (2021) performed a one-step prediction of ship motions under simulated oblique waves in sea state 8 using RNN, Gate Recurrent Unit (GRU), and LSTM. Xu et al. (2021) used LSTM to predict roll and heave motions under simulated irregular beam waves of sea state 7. Both studies chose wave height as the input feature to obtain information directly from the environment. However, these studies tested only one-step predictions, while the motion prediction for a future period is required in practice.

Until recently, few studies have focused on a multi-step prediction of the ship roll motion in high sea states. D'Agostino et al. (2021) investigated the short-term prediction of ship motions in stern-quartering sea state 7 based on CFD simulations, focusing on comparing the capabilities of RNN, GRU and LSTM. However, the selection of feature variables can still be further explored and refined. Inspired by the latest studies, this study focuses on the multi-step prediction of ship roll motions in high sea states, comprehensively investigating the effects of the feature variables and designing the specific learning algorithm.

This paper presents a novel data-driven method for the multi-step prediction of roll motions in high sea states. A neural network framework named ConvLSTMPNet is proposed to extract the nonlinear dynamic characteristics and the hydrodynamic memory information from wave heights and roll motions, in which LSTM and CNN are called in parallel. Taking the KCS ship model as the research object, the CFD method is utilized to generate the data in sea state 7 irregular long-crested waves with different encounter angles. A comparative study on the feature space demonstrates that selecting motion states and wave heights can improve prediction accuracy. LSTM and CNN algorithms are further adopted as contrasts. The results indicate the proposed method has better performance in predicting the amplitude of roll angles.

## 2. Problem description

The purpose of this study is to predict the ship roll motion in high sea states over a period of time, which helps the captain or autopilot obtain trends and make proper decisions to enhance operability and safety. In general, the roll motion in high sea states has large amplitudes and nonlinear dynamics. In this condition, the damping moment, the restoring moment, the added moment of inertia and the wave disturbance moment have more significant interaction effects than those at small roll angles, invalidating the assumption of the conventional

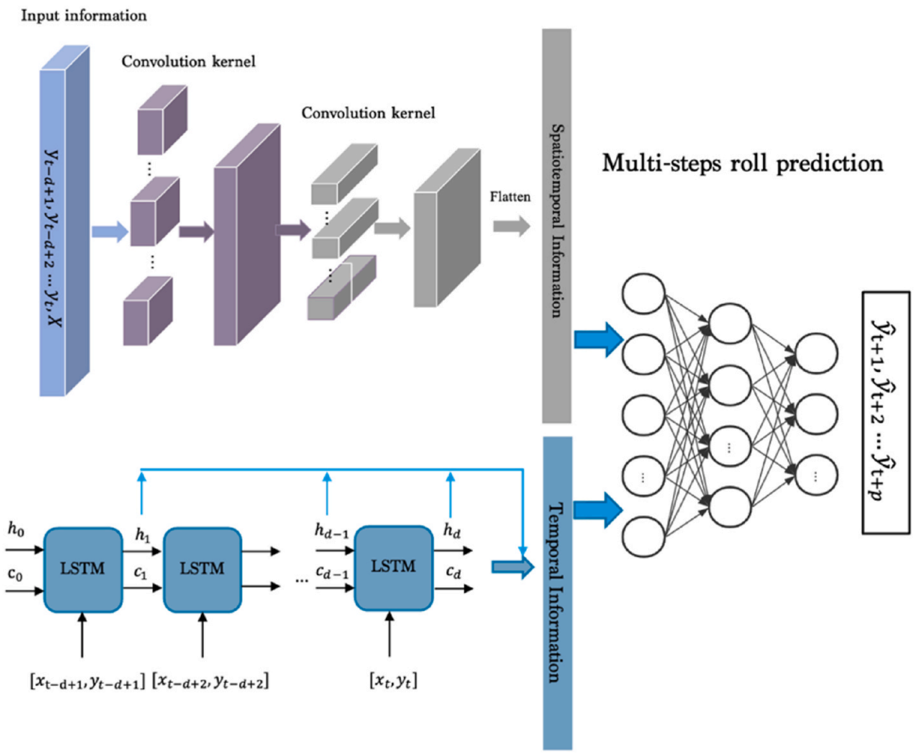


**Fig. 2.** Architecture of the ConvLSTMPNet.

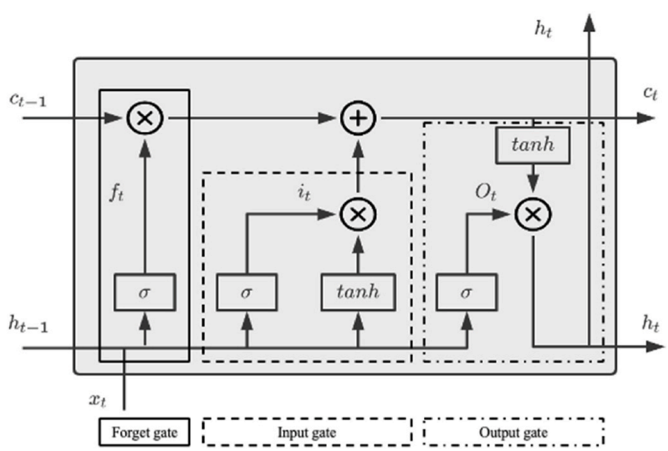


**Fig. 3.** Diagram of LSTM.

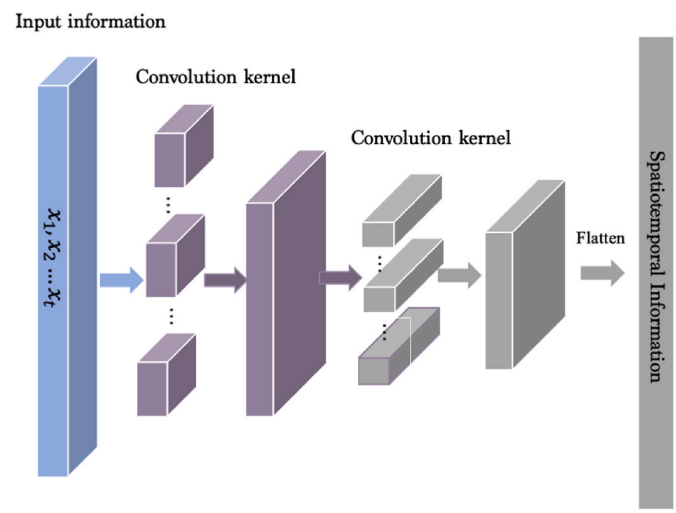


**Fig. 4.** The extraction of spatiotemporal information through 1D convolution.

mechanism models. Meanwhile, the interactions among the above-mentioned moments induce stronger nonlinearity. To construct hydrodynamic memory effects of ship roll motion in high sea state, a time series problem is considered and a multi-step prediction model will be developed by a data-driven approach.

Multi-step forecasting models predict a horizon of future values by all available inputs through a sequence-to-sequence architecture. It can be viewed as a modification of the one-step-head forecasting problem. In this study, the multi-step forecasting model of ship roll motion takes the form:

$$(y_{t+1}, y_{t+2}, \dots, y_{t+p}) = f(y_{t-d+1}, y_{t-d+2}, \dots, y_t, X_t) \tag{1}$$

where $(y_{t+1}, y_{t+2}, \dots, y_{t+p})$ is a discrete forecast horizon of roll angle, $(y_{t-d+1}, y_{t-d+2}, \dots, y_t)$ are the observations of the roll angle over a look-back window $d$ and $X_t = (x_{t-d+1}, x_{t-d+2}, \dots, x_t)$ are the exogenous inputs over a look-back window $d$. The $f(\cdot)$ is the nonlinear function to be learned. Thus, the forecasting modeling can be described as a supervised learning problem. The key issues are how to determine the feature variables and how to design the learning architecture to extract the information of nonlinear dynamics and hydrodynamic memory effects, thereby achieving accurate multi-step predictions.

## 3. Methodology

### 3.1. Overview of the methodology

The data-driven methodology mainly includes the design of the learning algorithm and the selection of feature variables. In addition, due to the specificity of the high sea state conditions, the data scarcity of the training set also needs to be considered.

**Table 1**
Dimension of KCS.

| Dimensions | Full Scale | Model Scale |
|---|---|---|
| Scale | 1 | 31.599 |
| Length between the perpendiculars(m) | 230 | 7.2786 |
| Beam at waterline(m) | 32.2 | 1.0190 |
| Depth(m) | 19 | 0.6013 |
| Draft(m) | 10.8 | 0.3418 |
| Displacement ($m^3$) | 52030 | 1.6490 |
| Longitudinal center of gravity from the aft(m) | 111.6 | 3.532 |
| Inertia moment of x axis/Beam at waterline | 0.4 | 0.40 |
| Inertia moment of z axis/Length between the perpendiculars | 0.26 | 0.26 |
| Design speed (m/s, full scale: kn) | 24 | 2.196 |
| Froude number | 0.26 | 0.26 |

**Fig. 5.** KCS hull model in STAR-CCM+.

**Table 2**
Classifications of wave level.

| Sea state | Significant wave elevation |
|---|---|
| 1 | <0.1 |
| 2 | 0.1–0.5 |
| 3 | 0.5–1.25 |
| 4 | 1.25–2.5 |
| 5 | 2.5–4.0 |
| 6 | 4.0–6.0 |
| 7 | 6.0–9.0 |
| 8 | 9.0–14.0 |
| 9 | >14.0 |

In terms of learning algorithms, to better extract the nonlinear dynamics and hydrodynamic memory effects of roll motions, a hybrid neural network is proposed that combines long short-term memory (LSTM) and convolutional neural network (CNN) in parallel, exploiting the CNN's ability to extract the multi-variable coupling relationships and the LSTM's ability to extract sequential correlation. As regards the feature variables, both roll motions and wave heights are investigated. To address the data scarcity of the training set, numerical computation through the CFD method is used to provide a high-fidelity dataset.

The overall procedure of the methodology is displayed in Fig. 1. Firstly, to address the data scarcity, the CFD method generates the ship motion data in high sea states with different wave directions. Secondly, the sliding window method is adopted to obtain the dataset suitable for supervised learning. Then, the proposed ConvLSTMPNet combined by CNN and LSTM network in parallel is used to extract nonlinear dynamics and hydrodynamic memory effect information, and the multi-step roll prediction is interpreted by the fully connected layers.

### 3.2. Multi-step forecasting model: ConvLSTMPNet

To express the hydrodynamic memory effects, a multi-step forecasting model for roll motion requires a sequence-to-sequence architecture. Therefore, it is important to extract sequential correlation efficiently. In addition, the forecasting model for roll motions involves multiple variables as inputs, such as the time history of roll angles and wave heights. Thus, it is also important to fuse the information from feature variables. Considering that LSTM and CNN have advantages in the above problems respectively, a parallel net of one-dimension CNN (Conv1D) and LSTM is designed, named ConvLSTMPNet.

A graphical illustration of the proposed model is shown in Fig. 2. The LSTM layer is used to learn the sequential correlation and the Conv1D layer is utilized to extract the local spatial-temporal information. They tackle the same inputs simultaneously. The outputs $C_t$ and $L_t$ of Conv1D and LSTM are connected end-to-end as inputs to the fully connected layer. Finally, the fully connected layer provides multi-step prediction results of the roll motions. The flow of information is presented in Eqs. (2)–(5):

$$C_t = g_1(W^c, [y_{t-d+1}, y_{t-d+2}, \ldots, y_t, X_t]) \tag{2}$$

$$h_m = g_2\left(W^h, [y_n, x_n, h_{m-1}]\right) \tag{3}$$

$$L_t = [h_1, h_2, \ldots, h_d] \tag{4}$$

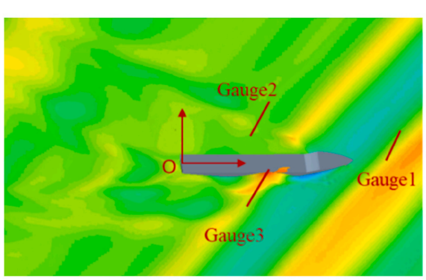


(a) The location of wave gauge near the hull.

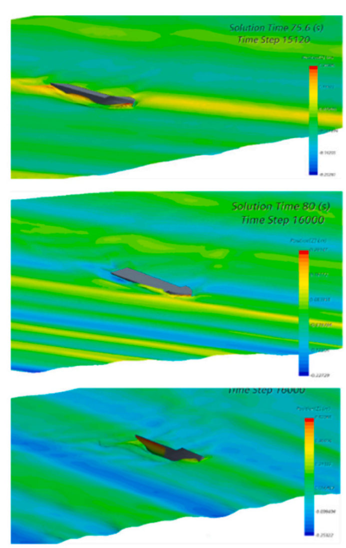


(b) From top to bottom, the wave heading angles are 150°, 120° and 90°, respectively

**Fig. 6.** Snapshots of the simulations.

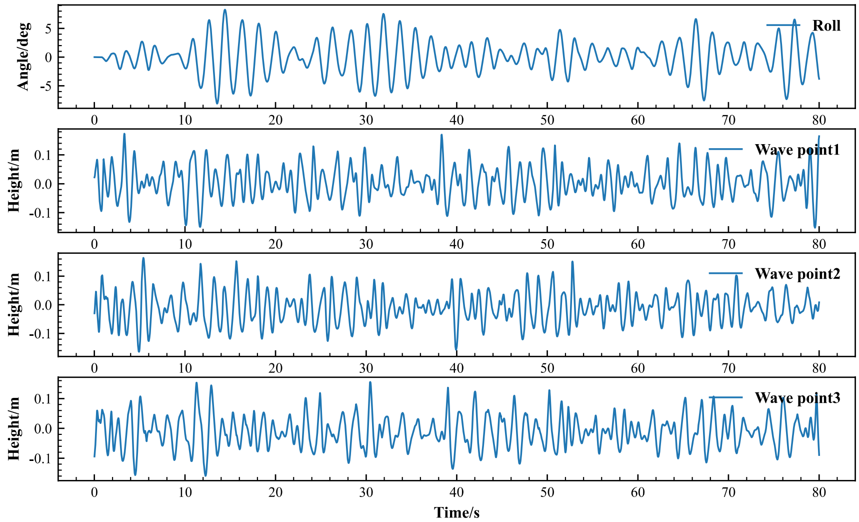


(a) Dataset #1: the wave heading angles of 150°

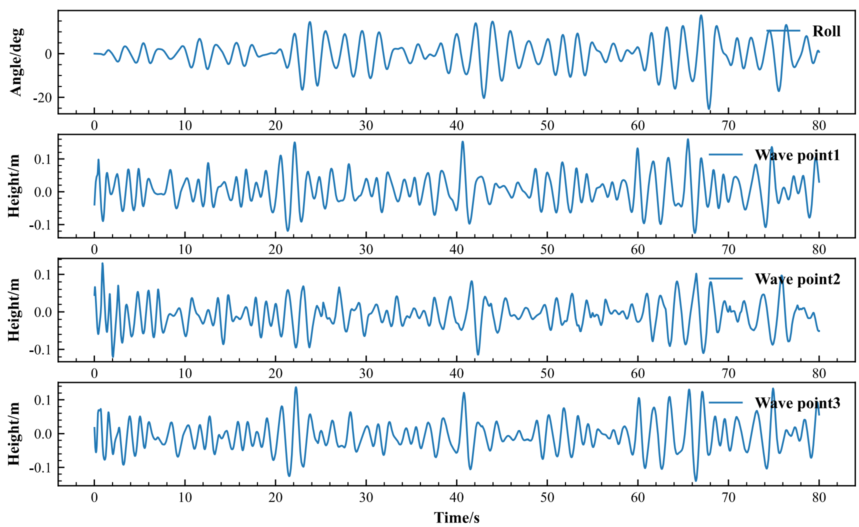


(b) Dataset #2: the wave heading angles of 120°

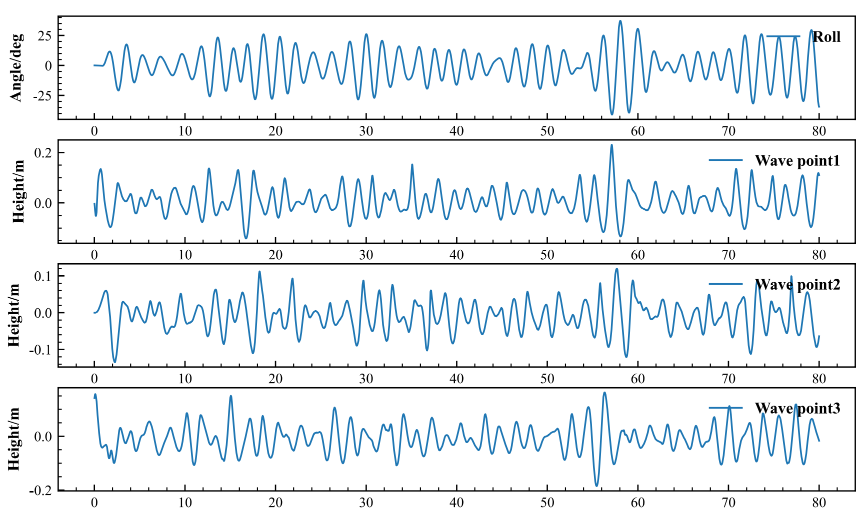


(c) Dataset #3: the wave heading angles of 90°

**Fig. 7.** Three simulated datasets in sea state 7.

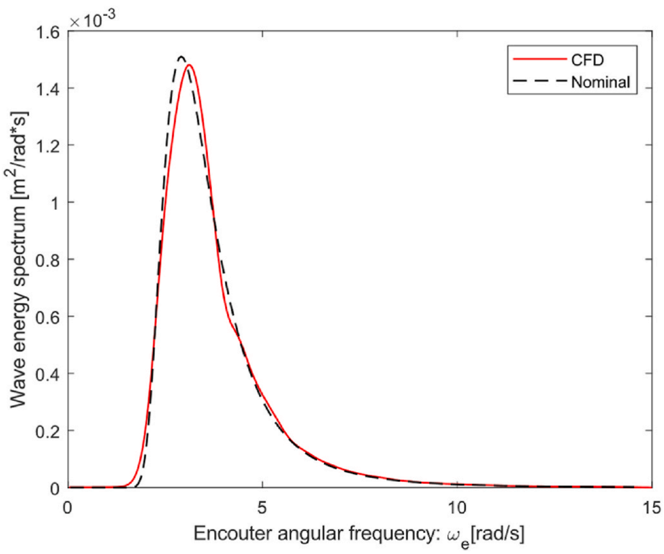


**Fig. 8.** Wave energy spectra of CFD results versus nominal results.

$$Y_t = (y_{t+1}, y_{t+2}, \ldots, y_{t+p}) = g_3(W^y, [C_t, L_t]) \tag{5}$$

where $W^c$, $W^h$ and $W^y$ represents the weights of Conv1D, LSTM, and the fully connected layers, $g_1(\cdot), g_2(\cdot)$, and $g_3(\cdot)$ represents nonlinear functions, $m = 1, 2, \ldots, d; n = t - d + 1, \ldots, t - d + 2, \ldots, t$. The hidden state sequence $[h_1, h_2, \ldots, h_d]$ is treated as the temporal information in LSTM layer.

Specifically, LSTM is a variate RNN where the gate cell is introduced to solve the problem of gradient vanishing and gradient explosion in RNN (Hochreiter and Schmidhuber, 1997), as shown in Fig. 3. The forget gate $f_t$ decides what to forget from the previous memory cell $c_{t-1}$. The input gate $i_t$ controls what to read out of the candidate memory cell $\widetilde{c}_t$ derived by state pair $[x_t, h_{t-1}]$, and $h_{t-1}$ is the previous hidden state. The output gate $o_t$ determines the value to be transferred into the next training. Therefore, the attribute of transferring the previous hidden state into next cycle and above gates can help it better capture the long-term dependencies of roll time series.

The corresponding formulas of LSTM are given in Eq. (6) to Eq. (11):

$$f_t = \sigma\left(W^{f,h}h_{t-1} + W^{f,x}x_t + b_f\right) \tag{6}$$

$$i_t = \sigma\left(W^{i,h}h_{t-1} + W^{i,x}x_t + b_i\right) \tag{7}$$

$$o_t = \sigma\left(W^{o,h}h_{t-1} + W^{o,x}x_t + b_o\right) \tag{8}$$

$$\widetilde{c}_t = tanh\left(W^{c,h}h_{t-1} + W^{c,x}x_t + b_c\right) \tag{9}$$

$$c_t = f_t \odot c_{t-1} + i_t \odot \widetilde{c}_t \tag{10}$$

$$h_t = o_t \odot tanh(c_t) \tag{11}$$

where $W^{f,h}, W^{f,x}, W^{i,h}, W^{i,x}, W^{o,h}, W^{o,x}, b_f, b_i, b_o$ represent the weight matrixes and bias of forget gate, input gate and output gate, respectively. In addition, $W^{c,h}$ and $b_c$ denote the weight matrix and bias of the candiate cell state respectively; $\sigma$ and $\odot$ are logistic sigmoid function and elementwise multiplication, respectively.

In ConvLSTMPNet, as shown in Fig. 2, the entire hidden state sequences of LSTM are used as outputs to provide more temporal information for fully connected layer, which is specifically designed for

**Table 4**
The mean and variance of the experimental and CFD data (illustrated as mean/variance).

| | $\lambda/L = 1.15$ | | $\lambda/L = 1.37$ | |
|---|---|---|---|---|
| | Exp | CFD | Exp | CFD |
| heave | −0.1494/0.333 | −0.159/0.312 | −0.051/0.3523 | −0.104/0.369 |
| pitch | −0.001/0.2822 | 0.0147/0.3059 | −0.0088/0.495 | 0.0072/0.4081 |
| wave | 0.1983/0.591 | 0.0584/0.503 | 0.0510/0.36 | 0.0192/0.476 |

**Table 3**
Wave energy spectrum moments of CFD and theorical results.

| Analysis CFD vs Theory | N.wave Comp. per run | Tot. run time/ $T_p$ | $m_0$ | | $m_1$ | | $m_2$ | |
|---|---|---|---|---|---|---|---|---|
| | | | Value [m$^2$] | E% | Value [m$^2$]rad/s | E% | Value [m$^2$] rad$^2$/s$^2$ | E% |
| Inputwave | 240 | 37 | 0.003055 | −0.00061% | 0.01149 | 0.0048% | 0.049561 | 0.0715% |

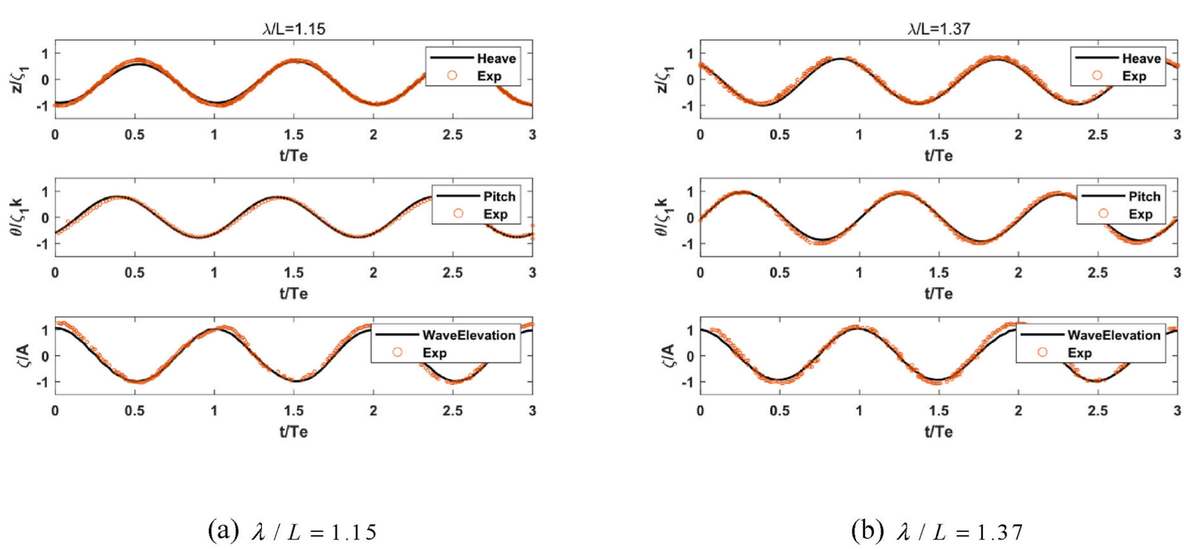


**Fig. 9.** The responses of KCS under regular waves.

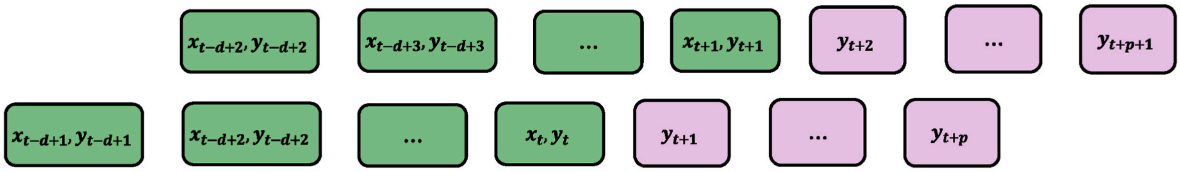


**Fig. 10.** Sliding window method.

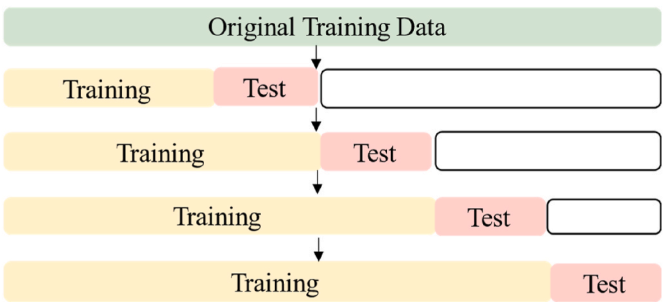


**Fig. 11.** Cross-validation on a rolling basis for time series prediction.

**Table 5**
Cross validation of optimal parameters on LSTM, CNN, ConvLSTMPNet.

| Candidate parameters | Model | | |
|---|---|---|---|
| | ConvLSTMPNet | LSTM | CNN |
| filters: [32,64,128] | 32,64 | None | 64,64 |
| hidden_units: [32,64,100,128] | 64 | 100 | None |

multi-step prediction.

A typical CNN contains convolutional layers, pooling layers, and fully connected layers. The convolutional layers can extract features from input sequences. The convolution kernel features the parameter sharing, thus reducing the number of weights to be trained and the complexity of the network. The pooling layers can distill the extracted features and pay attention to the most salient elements. The fully connected layers can interpret the internal representation to implement the task of regression or classification. Another important benefit of CNN is the support of multiple one-diemensional (1D) inputs as a separate channel to extract key information, i.e., the Conv1D layer. The one-dimension convolution operation is expressed in the following equation:

$$c(t) = (x * \omega)(t) = \sum_a x(t+a)\omega(a) \tag{12}$$

where $x$ is the input features; $t$ demotes the time; $\omega$ represents weights; $a$ is the position of convolution kernel, and $c$ is the feature map output after convolution operation $*$.

The CNN part in the ConvLSTMPNet is shown in Fig. 4. The 1D sliding convolution kernels move vertically to extract key spatiotemporal representation in the local time span from past time series of roll and wave elevation. Moreover, different convolution kernels can extract features from different perspectives to obtain higher-dimensional features. It is noted that no pooling layers are adopted due to the small data size compared to image data.

Finally, the spatiotemporal and the time dependency information from CNN and LSTM will be flattened and concatenated into one vector, then the multi-step prediction of roll motion can be interpreted by the fully connected layers.

### 3.3. Feature selection

The selection of feature variables is critical to the accuracy of roll motion prediction, because proper feature variables can enhance the upper bound of the forecast model performance. Generally, two types of variables have been selected to predict roll motions: motion states (Tang et al., 2021; Wei et al., 2021; Li, 2003) and wave elevations (Del Águila Ferrandis et al., 2021; Xu et al., 2021). The relevant studies have demonstrated that both the roll motion states and wave elevation can provide some information for the prediction of roll motions. Compared with one-step ahead predicting, the multi-step prediction has higher requirements for extracting sufficient information to ensure long-term accuracy.

Theoretically, if the data of motion states and wave heights involve different information, then the appropriate combination of these features can provide greater potential for forecasting modeling. However, few studies have investigated this problem. In this study, the time history of roll angles and the wave heights around ships are selected as feature variables. In Section 5.4, a comparative exploration of the feature selection is provided.

### 3.4. The generation of the numerical dataset

Datasets play a key role in model training and evaluation. However, available datasets for high sea states are scarce due to the high cost and navigational safety risks. In this study, a numerical technique based on computational fluid dynamics (CFD) is applied to obtain relatively high-fidelity data on ship motion in high sea states.

The datasets are generated by a Volume-of-Fluid (VOF) URANS solver in STAR-CCM+. Specifically, the VOF method is used to model the free surface. The superposed velocity and pressure fields of the individual regular waves are imposed as initial conditions to simulate irregular long-crested waves. Moreover, as the quality of the mesh is important for accurately simulating irregular waves, the adaptive mesh method is adopted to generate meshes of the free surface adaptively. The overset mesh method and Dynamic Fluid Body Interaction (DFBI) model is used to simulate ship motions, where pitch, heave and roll motions are collected. It should be noted that the long peak wave is a simplified treatment of irregular waves. Considering that the wave has a main direction in the actual sea, the application of long-crested waves can often obtain satisfied results in engineering.

The waves are assumed as stationary, homogeneous, and ergodic random process. Then, the elevation of irregular waves is represented through superposed regular waves as Eq. (13):

$$\zeta(t) = \sum_{i=1}^{n} a_i \cos(\omega_i t + \varepsilon_i) \tag{13}$$

where the $\zeta$ denotes wave elevation, $\omega_i$ is frequency of ith component wave, $\varepsilon_i$ is random phases between $-\pi$ and $\pi$ ,and the component wave amplitude $a_i$ for a given frequency is obtained from the following equation:

$$\frac{1}{2}{a_i}^2 \cong S(\omega_i)\Delta\omega_i \tag{14}$$

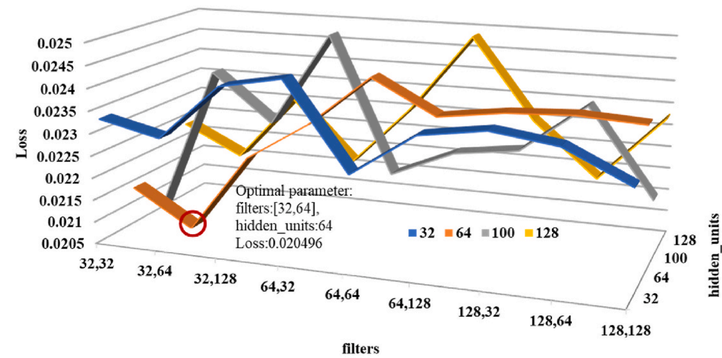


(a) Cross validation of parameters of ConvLSTMPNet

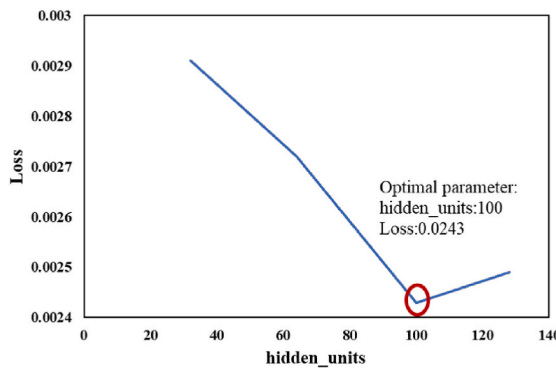


(b) Cross validation of parameters of LSTM

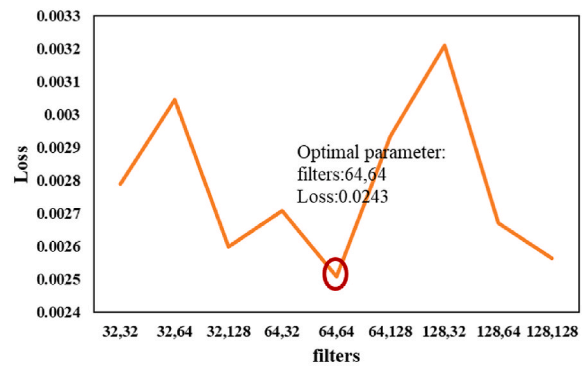


(c) Cross validation of parameters of CNN

**Fig. 12.** Cross validation of parameters of CNN, LSTM, ConvLSTMNet.

**Table 6**
Average RMSE of 10 steps and 20 steps roll prediction.

| Timesteps | 10 steps | | | 20 steps | | |
|---|---|---|---|---|---|---|
| Feature space | Roll angle | Wave elevation | Roll angle & Wave elevation | Roll angle | Wave elevation | Roll angle & Wave elevation |
| Dataset #1 | 1.17956 | 1.53057 | **0.69255** | 1.55123 | 1.51943 | **0.92316** |
| Dataset #2 | 3.47372 | 3.58599 | **2.69369** | 5.15763 | 4.15442 | **3.43608** |
| Dataset #3 | 3.03476 | 4.95515 | **1.20959** | 4.45659 | 2.79653 | **1.46759** |

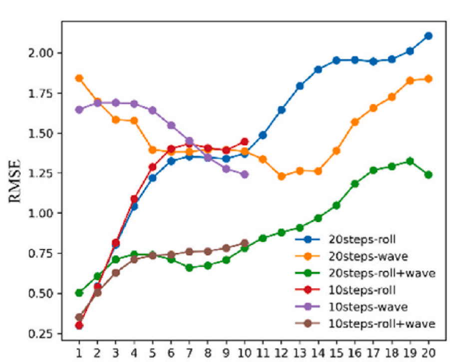


(a) dataset #1

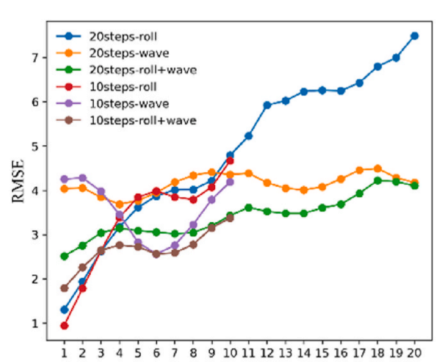


(b) dataset #2

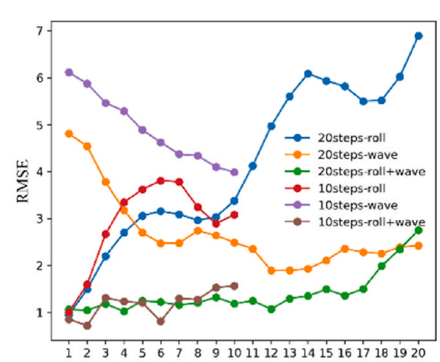


(c) dataset #3

**Fig. 13.** The RMSE of each step in multi-step prediction.

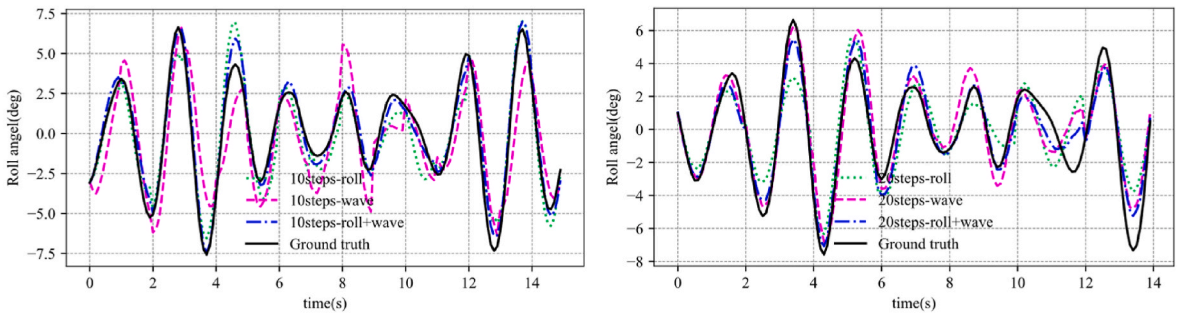


(a) Dataset#1

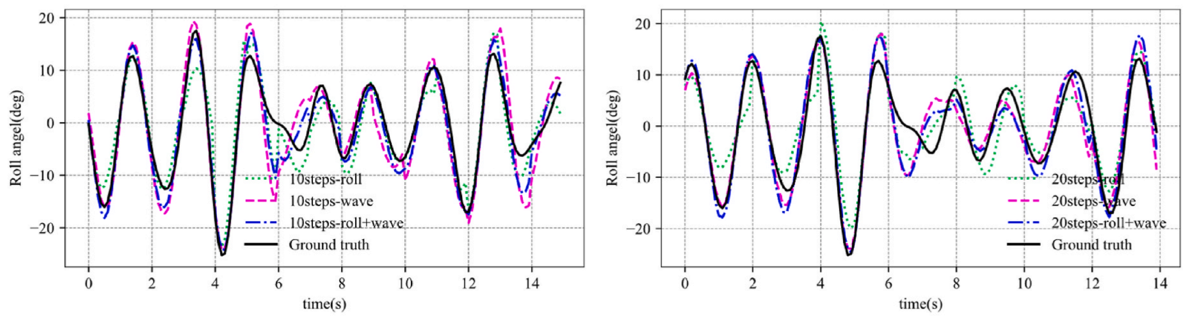


(b) Dataset#2

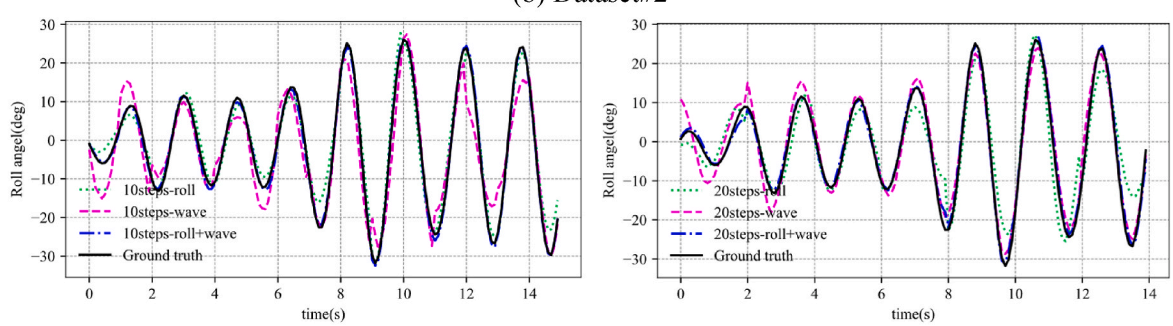


(c) Dataset#3

**Fig. 14.** The comparison results with different feature variables under dataset #1, #2 and #3.

**Table 7**
Average RMSE of CNN, LSTM and ConvLSTMPNet.

| Dataset | #1 | | | #2 | | |
|---|---|---|---|---|---|---|
| Model | CNN | LSTM | ConvLSTMPNet | CNN | LSTM | ConvLSTMPNet |
| Average RMSE | 1.05856 | 0.92316 | **0.80294** | 3.4442 | 3.43608 | **3.22126** |

$$S_{PM}(\omega) = \frac{5}{16}\left(H_s^{\,2}\omega_p^{\,4}\right)\omega^{-5}\exp\left(-\frac{5}{4}\left(\frac{\omega}{\omega_p}\right)^{-4}\right) \tag{15}$$

where $S_{PM}(\omega)$ is Pierson-Moskowitz (PM) spectrum, $H_s$ is significant wave elevation and $\omega_p = (2\pi/T_p)$ represents the angular peak frequency.

## 4. Data preparation and validation

### 4.1. Data generation

The KCS ship is taken as the study object. Considering the computational cost, the scale KCS ship model is adopted. The dimensions of the full scale and model scale KCS are given in Table 1 and the geometry of KCS is shown in Fig. 5. The extreme sea condition is selected as sea state 7. The Superposition of Wave method in the VOF module is adopted to generate irregular long-crested waves following the PM spectrum with 240 linear regular component waves at equal frequency intervals. Referring to the World Regulation of the State Oceanic Administration (Table 2), the specific wave parameters for the scale model in sea state 7 are set as follows: the significant wave height $H_s = 0.2215$ (corresponding 7 m in full scale) and the peak wave period $T_p = 2.16s$ (corresponding 12.13s in full scale).

Numerical datasets are constructed for three conditions with encounter angles of 150°, 120°, and 90°, called Dataset #1, Dataset #2, and Dataset #3, respectively. It is noted that the encounter angle of 90° corresponds to the port beam wave, 0° to the following wave, and 180° to the head wave. The total number of grid points is around 14,700,000. The ship motions are calculated over 80s for each case. The time step is set to 0.005s to satisfy the Courant-Friedrichs-Lewy condition. The time series of roll angles and the wave heights around the hull at three points are collected for training. In the CFD numerical tank, three wave gauges

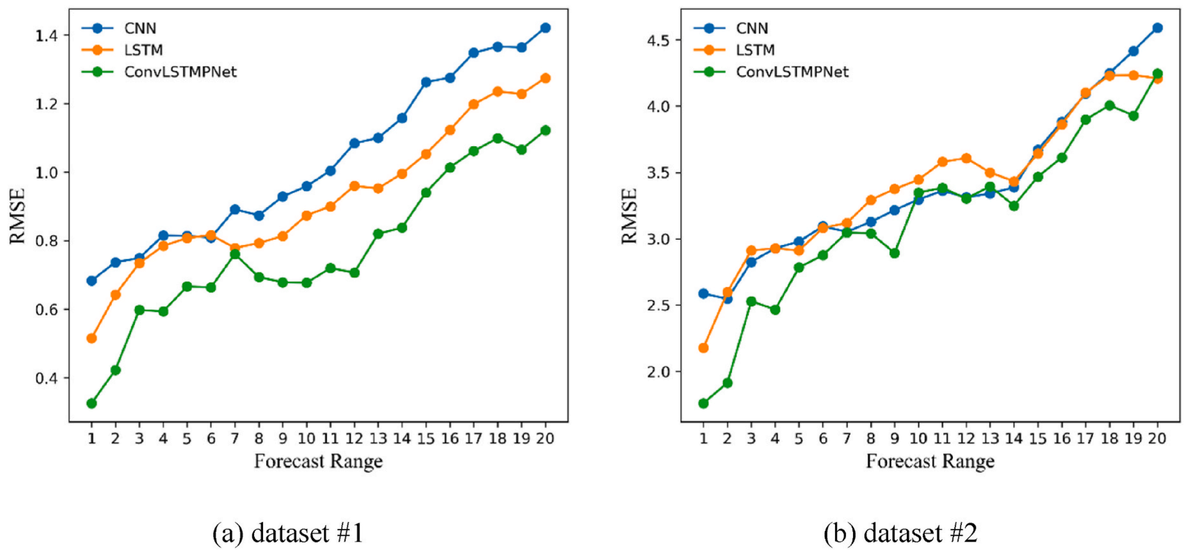


**Fig. 15.** The RMSE of each step in multi-steps prediction: (a) dataset #1; (b) dataset #2.

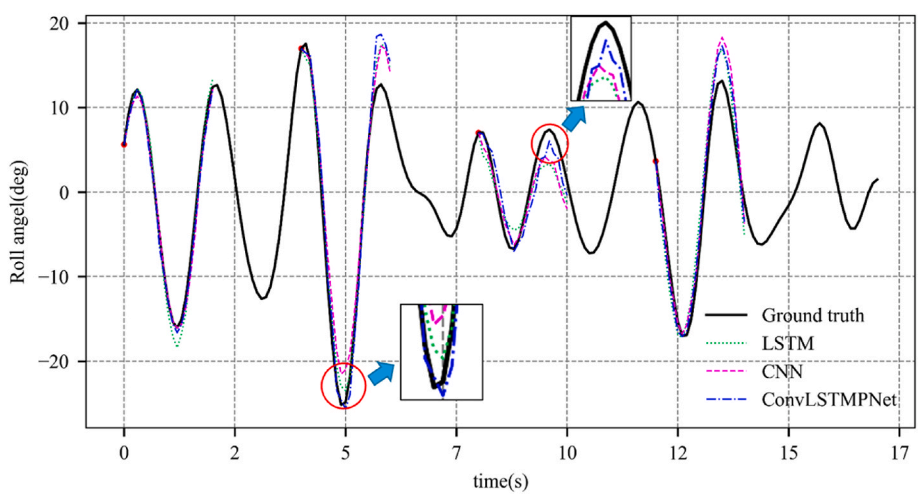


**Fig. 16.** The prediction results with CNN, LSTM and ConvLSTMPNet for dataset #2.

that monitor the free surface elevation are as shown in Fig. 6 (a). Gauge 1 is 0.2 times of ship length away from the bow, and Gauge 2 and 3 are 1.5 times of ship width from the hull to detect the encounter wave around the ship. The snapshot of the simulation is shown in Fig. 6 (b).

The roll responses exhibit different characteristics with different encounter angles of waves (as shown in Fig. 7). Specifically, a) when the ship encounters 90° beam waves, the amplitude of roll angles is the largest, up to 30°. b) when the ship encounters the oblique waves of 120° and 150°, the roll angles stand in [−20°,15°] and [−10°, 8°], respectively. However, the nonlinear characteristics of roll motions under oblique waves are more significant than those under beam waves. Theoretically, when the ship encounters beam waves, the encounter frequency is equal to the wave frequency in this study case. In the conditions of 120° and 150° oblique waves, the encounter frequency is larger than the wave frequency, leading to a higher frequency response than that of beam waves. Therefore, the theoretical analyzes are consistent with the simulation results.

### 4.2. Validation of numerical datasets

The validation of the input irregular wave refers to the literature (Diez et al., 2018). The irregular wave generated by CFD is validated versus theoretical benchmark values from the spectrum. In Fig. 8, the CFD spectrum is compared to the nominal spectrum. In addition, the wave energy spectrum moments $m_0$, $m_1$, and $m_2$ are applied as additional variables to evaluate the accuracy of the CFD wave energy spectrum, as Eqs. 16 and 17:

$$m_k = \int_0^{\infty} \omega^k S(\omega) d\omega \quad k = 0, 1, 2 \tag{16}$$

$$E = {m_k}^{(\mathrm{CFD})} - {m_k}^{(t)} \tag{17}$$

where the superscript “CFD” represents simulation value and $t$ represents theoretical values, and $E$ indicates the error of the CFD wave energy spectrum moments to theoretical values.

The wave energy spectral moments for CFD and theoretical are presented in Table 3. The average error $E$ is small with an average of 0.026%. The results demonstrate that the CFD wave energy spectrum achieves good agreement with theoretical values, verifying the effectiveness of input irregular waves generated by the CFD method.

To test the availability of numerical results for the interaction between ships and waves, the simulated KCS motions in regular waves are compared with the experimental data from the 2015 Tokyo Workshop

(T2015 Workshop). Fig. 9 shows the comparison results for the wave length-ship length ratio $\lambda/L = 1.15, 1.37$, the wave height-ship length ratio $H/L = 1/60$ and Froude number $Fr = 0.26$. The mean and variance of simulated and experimental results is listed in Table 4. The mean and variance of Exp and CFD differ little, indicating that the CFD results make a great agreement with experimental data.

## 5. Study case: multi-step prediction of the roll motion in sea state 7

### 5.1. Data processing

For multi-step prediction of ship roll motions, the dataset is divided into a training set and a validation set with a ratio of 8:2. The data are normalized in the interval (0, 1) to improve the convergence of the model. Furthermore, the structure of the training data for each time step is translated into a sliding window form, such as $\left[x_{t-d+1}, y_{t-d+1}, \ldots, x_t, y_t, \ldots, y_{t+p}\right]$, $\left[x_{t-d+2}, y_{t-d+2}, \ldots, x_{t+1}, y_{t+1}, \ldots, y_{t+p+1}\right]$ (as shown in Fig. 10). The green boxes represent the input sequence, and the pink boxes represent the output sequence that needs to be predicted.

### 5.2. Model setting

To optimize the hyperparameters of the proposed algorithm, cross-validation on a rolling basis is conducted. The specific mode is shown in Fig. 11. The original data for training is divided into k blocks. At the first turn, several blocks of data are used for training, and one block is used for testing. Then the current test block is concatenated as part of the training data for the next round. This process continues multiple times until the data is fully utilized. Finally, the average mean square error is used to evaluate the performance of the hyperparameter set.

The ConvLSTMPNet architecture contains an LSTM layer and two Conv1D layers. The number of convolution filters and neural units of hidden layers in LSTM and CNN are investigated by cross-validation on a rolling basis. The hyperparameter candidates of the convolution filter are set to [32, 64, 128] with a fixed kernel size of 3, and the neural units of the hidden layer in the LSTM are set to [32,64,100,128]. The parameters of three fully connected layers in ConvLSTMPNet are fixed as 100, 50, and the same number of units as the steps desired to be predicted. Based on the method of cross-validation on a rolling basis, the relatively optimal parameters of the above three models are obtained and listed in Table 5 and Fig. 12. Then these parameters are used to conduct the following case study in Sections 5.4 and 5.5.

Specifically, the ConvLSTMPNet architecture contains one LSTM with 64 units in the hidden layer and two Conv1D layers with 32 and 64 filters, with a kernel size of 3. The outputs of CNN and LSTM are concentrated together as the input for the three fully connected layers to generate the final prediction. In the three fully connected layers, the first and second layers have 100, 50 units, respectively, and the third layer has the same number of units as the steps desired to be predicted. Theoretically, the ConvLSTMPNet synthesizes the advantages of the two models. To evaluate its performance, LSTM and CNN are selected as the comparison model. The LSTM model has 100 units in its hidden layer, the same setup as the fully connected layers in the ConvLSTMPNet model. For the CNN model, two Conv1D layers with 64 filters and kernel sizes of 3, the flatten results are transferred into the fully connected layers which have the same setting as the ConvLSTMPNet model to predict the roll motions. The length of the lag time is set to be equal to the length of the time to be predicted. The batch size is set to 50 and the above model is optimized by Adam optimizer.

### 5.3. Model evaluation

For the evaluation of the model, it should be mentioned that the main objective to be achieved is prediction, rather than explanation. This is because the data-driven method has the advantage of mapping nonlinear features through supervised learning, but somehow lacks explainability. Therefore, the results are mainly analyzed and evaluated from the perspective of the prediction effects by the index of RMSE and the visualization of the prediction performance. Mean Square Error (MSE) is taken as the loss function for training, and Root Mean Square Error (RMSE) is taken to evaluate the performance of the predictive model. The formulas are given in Eq. (18) and Eq. (19), where n is the total number of samples, $y_i$ denotes the real value and $\hat{y}$ denotes the predict value.

$$MSE = \frac{\sum_1^n (y_i - \hat{y}_i)^2}{n} \tag{18}$$

$$RMSE = \sqrt{\frac{\sum_1^n (y_i - \hat{y}_i)^2}{n}} \tag{19}$$

### 5.4. Study case I: evaluating the feature space for the multi-step prediction of roll motions

The average RMSEs of 10- and 20-step predictions are listed in Table 6. Figs. 13 and 14 show the prediction results under different feature spaces. Fig. 13 presents the assessment of the predictive accuracy for each time step under different feature spaces, represented by RMSE. Fig. 14 shows the comparison results between the predicted and actual values for roll motion under different input features space, where the black line indicates actual value, and the dashed line denotes predicted values under different feature variables. The left column shows the prediction results for 10 steps, and the right column shows the prediction results for 20 steps.

From Fig. 14, the roll and wave elevation can provide some valid information for predicting the roll motions, respectively. However, in the case of roll motion as the feature space, underestimation of large amplitude occurs due to the lack of external wave disturbance. Overall, it can be seen from Fig. 13 that when the roll motion states are used as the feature variable, the prediction error increases with the number of steps. Whereas, when wave heights are used as the feature variable, the error decreases with the increasing number of steps. This result indicates that the information contained in the roll motion state may be limited compared to the wave height, while the wave height requires more steps as input to reflect the effect of waves on roll motions. The results of Figs. 13 and 14, and Table 5 indicate that the feature space containing wave elevation and roll motion states can provide more sufficient information than using only one of them. With the development of wave measurement techniques based on visual sensors (Bergamasco et al., 2021; Cang et al., 2019) and wave radars (Lyzenga et al., 2015; Wang et al., 2007), real-time acquisition of wave heights has become possible. It is recommended to use both wave elevation and roll motion state as feature variables to enhance the prediction of roll motions in extreme sea conditions.

### 5.5. Study case II: multi-steps roll motion prediction based on ConvLSTMPNet, CNN and LSTM

The effects of the learning algorithm are investigated in this section under the premise of selecting both the time history of motion states and wave elevation information as the feature space. As seen in Study Case 1, the 20-step prediction in oblique waves (for datasets #1 and #2) still has room for improvement as the complicated coupling between the ship roll motion and the waves. To enhance the extraction efficiency of multidimensional information, the proposed ConvLSTMPNet is applied and evaluated by comparing it with LSTM and CNN described in Section 5.2.

The average RMSEs of the datasets #1 and #2 are listed in Table 7 and the RMSE of each step in the multi-step prediction is shown in

Fig. 15. It can be found that ConvLSTMPNet has the best performance, with the lowest average RMSE of 0.80294 and 3.22126 under datasets #1, # 2, respectively. Additionally, for each step of the 20-step prediction, ConvLSTMPNet obtains the highest predictive accuracy. In contrast, the performance of LSTM is slightly worse than that of the proposed hybrid model, but better than that of CNN.

In Fig. 16, four points are selected at intervals for dataset #2 and each of the 20-step predictions is conducted, which is 2s for the scaled model and 11s for the full scale. The results demonstrate that at least one period of roll motion can be accurately predicted by using the proposed method. Compared with the single LSTM and CNN methods, the proposed method has better performance in the prediction of the amplitude of roll angles. From the perspective of architectural composition, the ConvLSTMPNet architecture combines the advantages of LSTM and CNN in parallel to extract time memory effects and nonlinear coupling interaction between incident waves and ship motions, resulting in more accurate multi-step prediction results. In summary, the results demonstrate the effectiveness of the proposed method for the multi-step prediction of roll motion in high sea states.

## 6. Conclusion and future work

In this paper, a data-driven methodology is proposed for the multi-step prediction of ship roll motion in high sea states. A hybrid neural network ConvLSTMPNet which combines the LSTM and Conv1D in parallel is exploited to extract the nonlinear dynamic characteristics and the hydrodynamic memory information from wave and roll motion states, so as to obtain accurate multi-step predictions. The numerical solutions of KCS in sea state 7 irregular long-crested waves with different wave directions are generated as datasets by the CFD method. The comparative study of feature selection demonstrates the superiority of selecting both motion states and wave heights as the feature space. The proposed method can accurately predict at least one period of roll motion in high sea states. The accurate prediction of roll motion can benefit the operation and safety of marine vessels and support the development of decision-making technologies for autonomous ships.

## CRediT authorship contribution statement

**Dan Zhang:** Methodology, Supervision, Funding acquisition. **Xi Zhou:** Conceptualization, Methodology, Validation, Visualization, Writing – original draft. **Zi-Hao Wang:** Conceptualization, Methodology, Supervision, Formal analysis, Writing – review & editing. **Yan Peng:** Formal analysis, Funding acquisition. **Shao-Rong Xie:** Formal analysis, Funding acquisition.

## Declaration of competing interest

The authors declare that they have no known competing financial interests or personal relationships that could have appeared to influence the work reported in this paper.

## Data availability

The data that has been used is confidential.

## Acknowledgment

This work is financially supported by the National Natural Science Foundations of China [Grant number: 61973208, 52101361, 61991415], the "Shuguang Program" 20SG40 supported by Shanghai Education Development Foundation and Shanghai Municipal Education Commission, and the program of shanghai academic research leader 20XD1421700.

## References

Bassler, C.C., 2013. Analysis and Modeling of Hydrodynamic Components for Ship Roll Motion in Heavy Weather (PhD Thesis). Virginia Polytechnic Institute and State University.
Bergamasco, F., Benetazzo, A., Yoo, J., Torsello, A., Barbariol, F., Jeong, J.-Y., Shim, J.-S., Cavaleri, L., 2021. Toward real-time optical estimation of ocean waves' space-time fields. Comput. Geosci. 147, 104666.
Cang, Y., He, H., Qiao, Y., 2019. Measuring the wave height based on binocular cameras. Sensors 19, 1338.
Chung, J.-S., Bernitsas, M.M., 1997. Hydrodynamic memory effect on stability, bifurcation, and chaos of two-point mooring systems. J. Ship Res. 41, 26–44.
Del Águila Ferrandis, J., Triantafyllou, M.S., Chryssostomidis, C., Karniadakis, G.E., 2021. Learning functionals via LSTM neural networks for predicting vessel dynamics in extreme sea states. Proc. Royal Soc. A 477, 20190897.
D'Agostino, D., Serani, A., Stern, F., Diez, M., 2021. Recurrent-type Neural Networks for Real-Time Short-Term Prediction of Ship Motions in High Sea State arXiv preprint arXiv:2105.13102.
Diez, M., Broglia, R., Durante, D., Olivieri, A., Campana, E.F., Stern, F., 2018. Statistical assessment and validation of experimental and computational ship response in irregular waves. J. Verif. Validation Uncertain. Quantification 3 (2).
Gokce, M.K., Kinaci, O.K., 2018. Numerical simulations of free roll decay of DTMB 5415. Ocean Eng. 159, 539–551.
Hochreiter, S., Schmidhuber, J., 1997. Long short-term memory. Neural Comput. 9, 1735–1780.
Huang, B.G., Zou, Z., Ding, W., 2018. Online prediction of ship roll motion based on a coarse and fine tuning fixed grid wavelet network. Ocean Eng. 160, 425–437.
Hou, X.-R., Zou, Z.-J., 2016. Parameter identification of nonlinear roll motion equation for floating structures in irregular waves. Appl. Ocean Res. 55, 66–75.
Inoue, S., Hirano, M., Kijima, K., Takashina, J., 1981. A practical calculation method of ship maneuvering motion. Int. Shipbuild. Prog. 28, 207–222.
Jiang, H., Duan, S., Huang, L., Han, Y., Yang, H., Ma, Q., 2020. Scale effects in AR model real-time ship motion prediction. Ocean Eng. 203, 107202.
Jiang, Y., Wang, X.-G., Zou, Z.-J., Yang, Z.-L., 2021. Identification of coupled response models for ship steering and roll motion using support vector machines. Appl. Ocean Res. 110, 102607.
Jiao, J., Chen, C., Ren, H., 2019. A comprehensive study on ship motion and load responses in short-crested irregular waves. Int. J. Nav. Archit. Ocean Eng. 11, 364–379.
Li, J., 2003. Ship Seakeeping Performance.
Lyzenga, D.R., Nwogu, O.G., Beck, R.F., O'Brien, A., Johnson, J., de Paolo, T., Terrill, E., 2015. Real-time estimation of ocean wave fields from marine radar data. In: 2015 IEEE International Geoscience and Remote Sensing Symposium (IGARSS), pp. 3622–3625.
Newman, J.N., 2018. Marine Hydrodynamics. The MIT Press.
Serani, A., Diez, M., Walree, F. van, Stern, F., 2021. URANS analysis of a free-running destroyer sailing in irregular stern-quartering waves at sea state 7. Ocean Eng. 237, 109600.
Sun, J., Hu, S.L.J., Li, H., 2021. Nonlinear roll damping parameter identification using free-decay data. Ocean Eng. 219, 108425.
Sutskever, I., Vinyals, O., Le, Q.V., 2014. Sequence to Sequence Learning with Neural Networks arXiv:1409.3215.
Tang, G., Lei, J., Shao, C., Hu, X., Cao, W., Men, S., 2021. Short-term prediction in vessel heave motion based on improved LSTM model. IEEE Access 9, 58067–58078.
T2015 Workshop [online] Available at: http://www.t2015.nmri.go.jp. (Accessed 17 November 2022).
Wang, F., Yuan, G., Lu, Z., 2007. Investigation of real-time wave height measurement using X-band navigation radar. In: 2007 International Conference on Wireless Communications, Networking and Mobile Computing. IEEE, Shanghai, China, pp. 980–983.
Wang, J., Zou, L., Wan, D., 2017. CFD simulations of free running ship under course keeping control. Ocean Eng. 141, 450–464.
Wei, Y., Chen, Z., Zhao, C., Tu, Y., Chen, X., Yang, R., 2021. A BiLSTM hybrid model for ship roll multi-step forecasting based on decomposition and hyperparameter optimization. Ocean Eng. 242, 110138.
Xu, W., Maki, K.J., Silva, K.M., 2021. A data-driven model for nonlinear marine dynamics. Ocean Eng. 236, 109469.
Yasukawa, H., Yoshimura, Y., 2015. Introduction of MMG standard method for ship maneuvering predictions. J. Mar. Sci. Technol. 20, 37–52.
Yin, J., Zou, Z., Xu, F., 2013. On-line prediction of ship roll motion during maneuvering using sequential learning RBF neuralnetworks. Ocean Eng. 61, 139–147.
Yumori, I., 1981. Real time prediction of ship response to ocean waves using time series analysis. In: OCEANS 81.Presented at the OCEANS, vol. 81, pp. 1082–1089.